Kinetics of Electrogenic Transport by the ADP/ATP Carrier

T. Gropp,* N. Brustovetsky,# M. Klingenberg,§ V. Müller,§ K. Fendler,* and E. Bamberg*¶

*Max-Planck-Institut für Biophysik, 60596 Frankfurt, Germany; #Department of Physiology, University of Minnesota, Minneapolis, Minnesota 55455 USA; §Universität München, Institut für Physikalische Biochemie, 80336 Munich, Germany; and ¶Johann Wolfgang Goethe-Universität, 60439 Frankfurt, Germany

ABSTRACT The electrogenic transport of ATP and ADP by the mitochondrial ADP/ATP carrier (AAC) was investigated by recording transient currents with two different techniques for performing concentration jump experiments: 1) the fast fluid injection method: AAC-containing proteoliposomes were adsorbed to a solid supported membrane (SSM), and the carrier was activated via ATP or ADP concentration jumps. 2) BLM (black lipid membrane) technique: proteoliposomes were adsorbed to a planar lipid bilayer, while the carrier was activated via the photolysis of caged ATP or caged ADP with a UV laser pulse. Two transport modes of the AAC were investigated, ATP_{ex}-0_{in} and ADP_{ex}-0_{in}. Liposomes not loaded with nucleotides allowed half-cycles of the ADP/ATP exchange to be studied. Under these conditions the AAC transports ADP and ATP electrogenically. Mg^{2+} inhibits the nucleotide transport, and the specific inhibitors carboxyatractylate (CAT) and bongkrekate (BKA) prevent the binding of the substrate. The evaluation of the transient currents yielded rate constants of 160 s^{-1} for ATP and $\geq$400 s^{-1} for ADP translocation. The function of the carrier is approximately symmetrical, i.e., the kinetic properties are similar in the inside-out and right-side-out orientations. The assumption from previous investigations, that the deprotonated nucleotides are exclusively transported by the AAC, is supported by further experimental evidence. In addition, caged ATP and caged ADP bind to the carrier with similar affinities as the free nucleotides. An inhibitory effect of anions (200–300 mM) was observed, which can be explained as a competitive effect at the binding site. The results are summarized in a transport model.

INTRODUCTION

The ADP/ATP carrier (AAC) is the most abundantly occurring transporter of the inner mitochondrial membrane and is responsible for the membrane potential-driven exchange of ATP versus ADP between the matrix space and the cytosol (Klingenberg, 1972, 1980). This process is the last step of oxidative phosphorylation. The function and the electrogenicity of the carrier have been investigated in detail mainly by flux measurements and binding studies on mitochondria, submitochondrial particles, and purified AAC reconstituted into liposomes (Klingenberg, 1985). By these techniques only steady-state transport studies were possible.

More recently we succeeded in measuring directly the currents generated by the ATP and ADP transport (Brustovetsky et al., 1996, 1997). Proteoliposomes were adsorbed to a planar lipid bilayer, and after a light-induced concentration jump of ATP (ADP) from the corresponding caged nucleotide, the resulting currents were recorded. These experiments directly suggested the electrogenicity of transport by the AAC. The six possible transport modes were investigated: ADP_{ex}-ATP_{in}, ATP_{ex}-ADP_{in}, ADP_{ex}-ADP_{in}, ATP_{ex}-ATP_{in}, ATP_{ex}-0_{in}, and ADP_{ex}-0_{in}. In the ATP_{ex}-ADP_{in} heteroexchange mode, net negative charge is transported into the liposomes, and in the ADP_{ex}-ATP_{in} mode it is transported out of the liposomes. However, transient currents could also be measured in the homoexchange modes (ADP_{ex}-ADP_{in}, ATP_{ex}-ATP_{in}) and with unloaded liposomes (ATP_{ex}-0_{in}, ADP_{ex}-0_{in}).

All of the electrical measurements made so far have been carried out by the adsorption of proteoliposomes to a planar lipid bilayer and applying nucleotide concentration jumps by photolysis of a caged substrate with a high-pressure mercury lamp (pulse duration 125 ms). Yet, there were two main points that could not be answered. First, which part of the electrical signal is due to the electrogenic transport of a nucleotide by the AAC and which part is due to the electrogenic release of the nucleotide from the caged nucleotide in the binding site? Second, what are the respective kinetics of the electrogenic ATP and ADP translocations?

To answer the first question we used a rapid solution exchange technique based on solid supported membranes that allows concentration jump experiments to be carried out without caged substrates. The second question could be solved by using a UV laser pulse (pulse duration 10 ns) instead of a UV lamp for the release of the caged nucleotides, so that the time resolution could be improved down to $\sim$500 μs. To investigate the steps of ATP and ADP transport in detail with an experimental system that is as simple as possible, we used unloaded liposomes (ATP_{ex}-0_{in} and ADP_{ex}-0_{in}). This system allows one to study a half-cycle of the ATP/ADP exchange. For the first time it is possible to give an estimation of the reaction rates of the electrogenic transport of ATP and ADP by the AAC. A transport model based on these results is proposed.

Received for publication 8 December 1998 and in final form 4 May 1999.

Address reprint requests to Dr. Ernst Bamberg, Max-Planck-Institut für Biophysik, Kennedyallee 70, 60596 Frankfurt, Germany. Tel.: +49-69-6303-300/301; Fax: +49-69-6303-305; E-mail: bamberg@biophys.mpg.de.

0006-3495/99/08/714/13 $2.00

MATERIALS AND METHODS

BLM experiments

Electrical currents of the AAC were measured by adsorption of AAC-containing proteoliposomes to a black lipid membrane (BLM) as described elsewhere (Brustovetsky et al., 1996). The black lipid membranes, with an

area of 1.3 mm^2, were formed in a Teflon cell filled with an electrolyte containing 100 mM NaCl and 20 mM 2-(*N*-morpholino)ethanesulfonic acid (MES) (pH 6.2) (if not otherwise stated). The high buffer concentration was used to avoid the fast protonation of the bilayer, which can also yield a transient current. Each compartment of the Teflon cell has a volume of 1.5 ml. The membrane-forming solution contained 1.5% (wt/vol) diphytanoylphosphatidylcholine and 0.025% (wt/vol) octadecylamine in *n*-decane to obtain a positively charged membrane surface (Dancshazy and Karvaly, 1976). Membrane formation was controlled by eye, and the capacitance of the membrane was determined (for further details see Bamberg et al., 1979). The temperature was kept at 24°C, and because there is virtually no UV light absorption by the BLM and the liposomes, the local temperature is not influenced by the laser flash.

The purified AAC from bovine heart mitochondria was reconstituted into liposomes (95% phosphatidylcholine, 5% cardiolipin) with a final protein concentration of 0.4 mg/ml and a protein-to-lipid weight ratio of 0.02 (Krämer, 1986; Brustovetsky et al., 1996, 1997). Fifteen microliters of the proteoliposome-containing suspension was added to the compartment of the cuvette opposite the light source. Under stirring, the adsorption of the liposomes to the BLM took ~90 min. Then caged ATP or caged ADP (P^3-1-(2-nitrophenyl)ethyl ester of ATP or ADP) was added to the suspension.

The caged nucleotides were irradiated by a UV light pulse of an excimer laser (wavelength 308 nm, pulse duration 10 ns), which was focused on the BLM. Approximately 0.8 mm^2 of the BLM was exposed to the laser beam. The average radiant exposure on the BLM surface was 150 mJ/cm^2, which yields an η (fraction of nucleotide released from caged analog) of 26%. As was shown in earlier publications, no significant temperature change ($\Delta T < 1$°C) that could influence the current signal is caused by the illumination of the BLM (Knoll and Stark, 1977). This is supported by the fact that in the experiments presented in this publication, at varying radiant exposures in the range of one order of magnitude, no effect on the kinetics of the carrier was observed.

The transient current generated by the AAC was amplified (10^9-fold), filtered (1 kHz with a first-order low-pass filter), and recorded with a digital oscilloscope. Because of the capacitive coupling of the AAC to the electrical circuit, an additional exponential function with a system time constant τ_0 is expected in the signal (Bamberg et al., 1979; Borlinghaus et al., 1987): $\tau_0 = (C_m + C_p)/(G_m + G_p)$ ($C_{m/p}$ = specific capacitance of the BLM/liposomes, $G_{m/p}$ = specific conductivity of the BLM/liposomes).

The fraction of released ATP was determined with a luciferin-luciferase assay as described previously (Nagel et al., 1987). For the fraction of released ADP from caged ADP, ADP was first converted to ATP by creatine phosphokinase and phosphocreatine, and then the ATP concentration was determined by the luciferin-luciferase assay. For both caged ATP and caged ADP the amount of released nucleotide was the same for a given radiant exposure.

The time constants for the ATP and ADP release were measured spectroscopically as described by Walker et al. (1988). For this purpose the formation and decay of an aci-nitro compound during the release of the caged nucleotide were observed at a wavelength of 406 nm. The values of the time constants at different pH and Mg^{2+} concentrations are given in Tables 1 and 2; these are in the same range as the values found by Walker et al. for the release of ATP. The release rates depend on the Mg^{2+} concentration and on the pH. At high Mg^{2+} concentration the release of the nucleotides was slower. This effect was more pronounced in the case of ATP, probably because of the higher binding affinity for Mg^{2+} (pK 4.06 (ATP), pK 3.17 (ADP); Martell and Smith, 1974). At varying pH the release rate was increased by a factor of $10^{\Delta pH}$, which is in agreement with theory (Walker et al., 1988). The activation energies for the release of ATP and ADP were 60 kJ/mol and 57 kJ/mol, respectively.

Fast solution exchange on a solid supported membrane

In addition to the bilayer experiments, we applied a fast fluid injection technique, which allows the measurement of electrical currents generated by the AAC, using a solid supported membrane (SSM) (Pintschovius and Fendler, 1999).

The advantage of this technique is that concentration jumps of an arbitrary substrate (i.e., ADP or ATP) can be performed with a time resolution of up to 10 ms without the use of caged substrates.

Solid supported membranes consist of an alkanethiol monolayer on a gold electrode combined with an additional layer of phospholipid on top. The resulting double layer can be used in a way similar to that of the BLM. The electrical properties of the SSM and the BLM are similar. The capacitance of the SSM was typically 400 nF/cm^2, and the conductance 100 nS/cm^2. The high conductivity of the SSM compared to the BLM (3 nS/cm^2) is probably due to defect structures on the large surface of the SSM (4–5 mm^2). The SSM is positioned in a plexiglass cuvette with an inner volume of 17 μl, which allows a fast exchange of the solutions.

Furthermore, the concentration rise over the SSM had to be taken into account. The nucleotide concentrations were corrected as described by Pintschovius and Fendler (1999), so that the resulting concentration was $c_{korr.} \approx 0.5c_0$.

The AAC-containing proteoliposomes were adsorbed to the SSM. The carrier was activated by a rapid solution exchange over the SSM. The rapid solution exchange was performed by driving two syringes with a perfusor pump. The two syringes contained the activating and nonactivating solutions, and the fluid flow was controlled by an electrical valve. The resulting electrical current was amplified by an operational amplifier and a low-noise amplifier 10^9-10^{10}-fold, filtered (300 Hz, low-pass), and recorded. The carrier was activated via solution exchange for 2 s from $t = 6$ s to $t = 8$ s. The short peaks at $t = 6$ s and $t = 8$ s are artefacts and are caused by the turning on and off of the electrical valve. At $t < 6$ s and $t > 8$ s nonactivating solution was flowing through the mixing chamber.

RESULTS

Unloaded liposomes (ATP_{ex}-0_{in}, ADP_{ex}-0_{in}) were used to investigate half-cycles of the ATP/ADP exchange. Two techniques were applied to perform ATP or ADP concentration jumps: a fast solution exchange on an SSM and the photolytic release of nucleotides with the BLM method. The purpose of the SSM measurements was 1) to determine in a control experiment whether ATP and ADP translocation or binding, respectively, are electrogenic and to investigate the influence of the photolytic release of these nucleotides; 2) to

TABLE 1 Comparison of the time constants of the transient currents from ADP translocation at different pH with spectroscopic data of the nucleotide release: pH dependence of the relaxation time constants for ADP_{ex}-0_{in} and spectroscopic data of the ADP release at 0 and 4 mM Mg^{2+}

pH	τ_1 (ms)	ADP rel. (ms) 0 Mg^{2+}	τ_2 (ms)	$\tau_{1,Mg^{2+}}$ (ms)	ADP rel. (ms) 4 mM Mg^{2+}
6.2	2.3	0.9	10.6	2.1	1.1
6.4	3.3	1.6	31.8		2.0
6.65	4.2	2.9	36.3	2.9	3.5
7.0	4.7	5.8	21.7	7.5	6.8

TABLE 2 Comparison of the time constants of the transient currents from ATP translocation at different pH with spectroscopic data of the nucleotide release: pH dependence of the relaxation time constants for ATP_{ex}-0_{in} and spectroscopic data of the ATP release at 0 and 4 mM Mg^{2+}

pH	τ_1 (ms)	ATP rel. (ms) 0 Mg^{2+}	τ_2 (ms)	τ_3 (ms)	$\tau_{1,Mg^{2+}}$ (ms)	ATP rel. (ms) 4 mM Mg^{2+}
6.2	1.0	0.9	6.7	26.5	1.7	1.8
6.45		1.4			3.7	3.4
6.7		2.9				6.1
7.05		6.7			10.9	11.6
7.2	6.3		8.3	55.8		

Conditions: 100 mM NaCl, 20 mM MES, 500 μM caged ADP/caged ATP respectively; $T = 24°C$; $\eta = 26\%$.

investigate the behavior of the AAC on addition and removal of the nucleotides (on-response and off-response); and 3) to compare with the results obtained by the BLM experiments. The BLM technique was used to investigate the kinetic properties of the AAC by laser-induced nucleotide concentration jumps.

Current measurements on solid supported membranes

ADP and ATP Transport and inhibition

In Fig. 1, *A* and *C*, the currents induced by concentration jumps of 100 μM ADP and 100 μM ATP are shown. The fluid flow with the nucleotide-containing solution was started at $t = 6$ s and stopped at $t = 8$ s, causing a short artefact due to the switching of the electrical valve. After a delay time of ~100 ms, which is the traveling time of the fluid from the electrical valve to the cuvette, an on-response as well as an off-response could be detected. In the case of ATP_{ex}-0_{in}, the positive on-response corresponds to the transport of negative charge into the liposomes and the negative off-response to the transport of negative charge out of the liposomes. In the case of ADP_{ex}-0_{in} the currents are reversed. The on-response corresponds to the transport of negative charge out of the liposomes and the off-response to the transport of negative charge into the liposomes. Fig. 1 *B* shows the inhibition of the ADP-induced current by 1 μM carboxyatractyloside (CAT) and 1 μM bongkrekic acid (BKA). CAT and BKA act as specific inhibitors and bind to the cytosolic and matrix sides of the AAC, respectively (Brustovetsky et al., 1996; Fig. 11 *A*). Similar results were obtained for ATP-induced currents (data not shown).

Mg^{2+} forms a complex with ATP and ADP that cannot be transported (Klingenberg, 1980). This is demonstrated for ATP in Fig. 1 *D*. Inhibition of ATP and ADP transport by Mg^{2+} was also found in the BLM experiments (Fig. 3). After the addition of 4 mM $MgCl_2$ to the activating solution, no electrical current could be detected.

Transported charge

We observed charge translocation induced by an ADP and ATP concentration jump (on-response), but also a charge movement in the opposite direction with removal of the nucleotides (off-response). The transported charges for the on- and off-responses were calculated by integrating the signals and are approximately the same. At least 80–90% of the charge transported into the liposomes on activation with the nucleotides is transported back out of the liposomes on removal of the nucleotides. Comparison of the transported charge in the on-response of the ATP_{ex}-0_{in} transport and ADP_{ex}-0_{in} transport in the same experiment yielded a ratio of ~2:1. This implies that during translocation of one ATP molecule twice as much charge is moved compared to the translocation of one ADP molecule. A similar result was found at pH 7.4 (data not shown).

Dependence on the ATP concentration

The ATP dependence of the peak current of the on-response was measured as shown in Fig. 2. In this figure the ATP concentration was corrected for the limited concentration rise according to Pintschovius and Fendler (1999). The data can be fitted with a hyperbolic function that yields a half-saturating concentration of $K_{0.5} = 60$ μM for ATP.

Current measurements on black lipid membranes

In the BLM experiments the transport through AAC is activated via photolysis of caged ATP or caged ADP. With this method ~20–30% of ATP or ADP is released with a time constant of ~1 ms (pH 6.2) after the laser flash (Tables 1 and 2).

ADP and ATP transport and inhibition by Mg^{2+}

The shape of the recorded currents is complex, so that, for reasons of simplicity, we will divide the current traces into different phases. In Fig. 3 *A* an ATP concentration jump experiment (*upper trace*) is depicted. The current consists of two phases, each one of which consists of a rise and a decay. The fast phase occurs within the first 2 ms and is not time resolved. It will be called the fast-release phase (frp). As will be shown below, it corresponds to a fast process in connection with the release of ATP. The slower phase takes ~50 ms and will be called the transport phase (tp) because it presumably corresponds to the transport of the nucleotide. The sign of the current reflects the movement of negative charge into the liposomes. The rise of the transport phase is

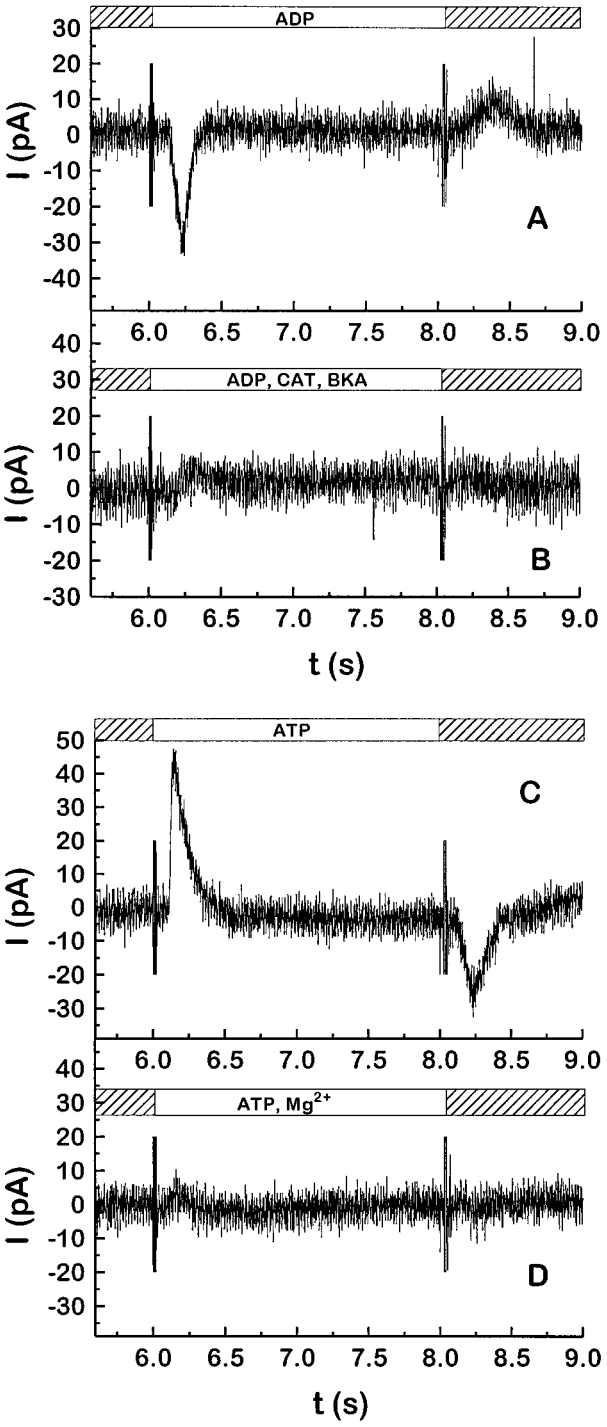

FIGURE 1 SSM experiment: ADP and ATP concentration jump and inhibition of the AAC transport activity. (*A*) Activating solution: 100 mM NaCl, 20 mM MES (pH 6.2), 100 μM ADP; nonactivating solution: 100 mM NaCl, 20 mM MES (pH 6.2). (*B*) Activating solution: 100 mM NaCl, 20 mM MES (pH 6.2), 100 μM ADP, 1 μM CAT, 1 μM BKA; nonactivating solution: 100 mM NaCl, 20 mM MES (pH 6.2). (*C*) Activating solution: 100 mM NaCl, 20 mM MES (pH 6.2), 100 μM ATP; nonactivating solution: 100 mM NaCl, 20 mM MES (pH 6.2). (*D*) Activating solution: 100 mM NaCl, 20 mM MES (pH 6.2), 100 μM ATP, 4 mM $MgCl_2$; nonactivating solution: 100 mM NaCl, 20 mM MES (pH 6.2), 4 mM $MgCl_2$. $T = 24$°C.

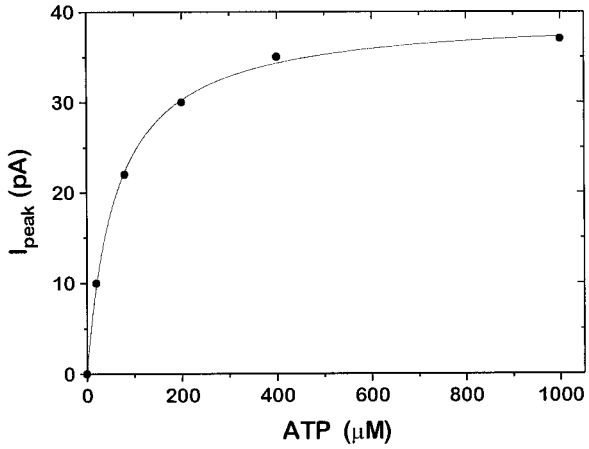

FIGURE 2 SSM experiment: peak current of an ATP on-response at increasing ATP concentration; for conditions see Fig. 1. The ATP concentration is corrected according to Pintschovius et al. (1999). The half-saturating concentration is 60 μM.

characterized by τ_1 and the decay by τ_2 and τ_3. The rise of the transport phase could be resolved to a different extent in various experiments. In some cases the fast-release phase and transport phase overlap, so that the decay of the transport phase directly follows the decay of the fast-release phase. The time constants of the decay of the transport phase are not influenced by this effect. In the presence of 2 mM $MgCl_2$ (*lower trace*, Fig. 3 *A*), the transport phase is blocked in the same way as in the SSM experiments, but an additional negative overshoot appears, which we call the slow-release phase (srp). It is also related to the release of ATP (see below) and corresponds to the movement of negative charge out of the liposomes. The decay of the slow-release phase is characterized by $\tau_{1,Mg^{2+}}$.

A similar experiment is shown in Fig. 3 *B*. The lower trace represents the activation of the AAC by photolysis of caged ADP. Again, the fast positive phase will be called the fast-release phase. Because the transport phase has an opposite sign compared to ATP_{ex}-0_{in}, the following negative phase is an overlap of the slow-release phase and the transport phase. The decay of the transport phase is characterized by τ_1 and τ_2. After the addition of $MgCl_2$ (*upper trace*, Fig. 3 *B*), the amplitude of the slow-release phase plus the transport phase is significantly smaller, and we will call this remaining phase the slow-release phase. The decay of the slow-release phase is characterized by $\tau_{1,Mg^{2+}}$. It should be noted that the current traces after the addition of Mg^{2+} in the case of ADP_{ex}-0_{in} and ATP_{ex}-0_{in} are almost identical.

Electronic artefacts in the electrical currents, particularly in connection with the fast-release phase and the slow-release phase, were ruled out. In either case (ATP_{ex}-0_{in}, ADP_{ex}-0_{in}) all three phases of the signals can be blocked by CAT and BKA (Fig. 3, *C* and *D*). With the exception of the slow-release phase in the case of ATP_{ex}-0_{in}, inhibition could also be achieved by increasing the anion concentration. After the inhibition the remaining part of the fast-release phase is a laser artefact (Figs. 7 and 8), which is not related to the protein.

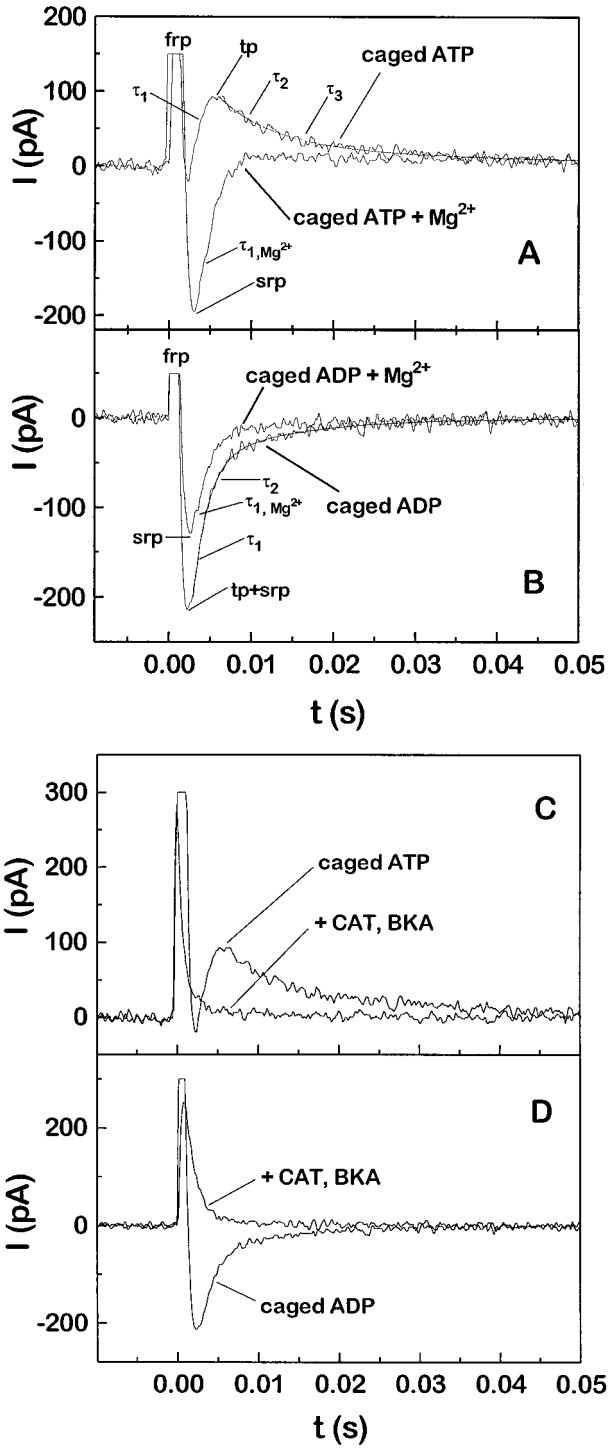

FIGURE 3 BLM experiment. (*A*) 100 mM NaCl, 20 mM MES (pH 6.2). *Upper trace*: 400 μM caged ATP; time constants: τ_1 = 1.0 ms, τ_2 = 6.4 ms, τ_3 = 30 ms. *Lower trace*: 400 μM caged ATP, 2 mM $MgCl_2$. (*B*) 100 mM NaCl, 20 mM MES (pH 6.2). *Upper trace*: 200 μM caged ADP; time constants: τ_1 = 1.8 ms, τ_2 = 11 ms. *Lower trace*: 200 μM caged ADP, 4 mM $MgCl_2$; T = 24°C; fraction of released nucleotide (η) = 26%. frp, fast-release phase; srp, slow-release phase; tp, transport phase. (*C* and *D*) Inhibition of the carrier with 5 μM CAT and BKA.

Our main interest is focused on the time constants that presumably characterize the rate-limiting steps in nucleotide transport and nucleotide release in the binding site (see Discussion). These relevant time constants (Fig. 3) are found in the decay of the transport phase of ADP_{ex}-0_{in} (τ_1 = 1.8 ms, τ_2 = 11 ms) and ATP_{ex}-0_{in} (τ_2 = 6.4 ms, τ_3 = 30 ms) signals and in the rise of the transport phase in the case of ATP_{ex}-0_{in} (τ_1 = 1.0 ms).

pH dependence

The rate constants for the release of nucleotides are significantly pH dependent and can be determined spectroscopically (see Materials and Methods; Walker et al., 1988). To find out which of the time constants in the BLM signals corresponds to the release of nucleotides from the caged analogs, we recorded AAC-induced transient currents at varying pH and compared the values for the time constants with the spectroscopic data of the nucleotide release. The results of these experiments are shown in Tables 1 and 2. In both cases, ATP_{ex}-0_{in} and ADP_{ex}-0_{in}, τ_1 and $\tau_{1,Mg^{2+}}$ were found to be significantly pH dependent. The time constants for nucleotide release determined by spectroscopic experiments (column ATP rel./ADP rel.) show a pH dependence similar to that of τ_1 and $\tau_{1,Mg^{2+}}$.

Dependence on ATP and ADP concentration

Fig. 4 shows the dependence of the peak current on the ATP and ADP concentration together with the time constants of the decay of the transport phase. The caged ATP (Fig. 4, *A–C*) and caged ADP (Fig. 4, *D–F*) concentrations were increased from 5 μM up to 2 mM while the laser energy was constant and yielded a fraction of released nucleotide (η) of 30% (*filled circles*). Alternatively, in a second step of the experiment the caged nucleotide concentration was kept constant at 2 mM and η was decreased from 30% to 0% by reducing the laser energy (*open circles*).

The peak current at increasing ATP concentration (Fig. 4 *A*, *filled circles*) follows a hyperbolic saturation curve. At variable η (*open circles*) a linear behavior of the peak current was observed. On the other hand, the time constants τ_2 and τ_3 remained approximately constant in both cases (Fig. 4, *B* and *C*). As average values for the two relaxation times we obtained $\tau_2 \approx 6$ ms and $\tau_3 \approx 30$ ms. The amplitude (A_2) of τ_2 (Fig. 5 *A*) shows the same dependence as the peak current in Fig. 4 *A*, whereas the amplitude (A_3) of τ_3 (Fig. 5 *B*) remains approximately constant. The ADP dependence of both the amplitudes (Fig. 5, *C* and *D*) and the time constants (Fig. 4, *E* and *F*) shows the same qualitative behavior as in the case of ATP_{ex}-0_{in}. The average relaxation times in the decay of the overlapping transport phase and slow-release phase are $\tau_1 \approx 2.7$ ms and $\tau_2 \approx 34$ ms.

Activation energy of the reactions

Fig. 6 shows the Arrhenius plots for the time constants. The activation energies are $E_A(\tau_2)$ = 71 kJ/mol, $E_A(\tau_3)$ = 50 kJ/mol for ATP_{ex}-0_{in}, and $E_A(\tau_1)$ = 46 kJ/mol, $E_A(\tau_2)$ = 29 kJ/mol for ADP_{ex}-0_{in}.

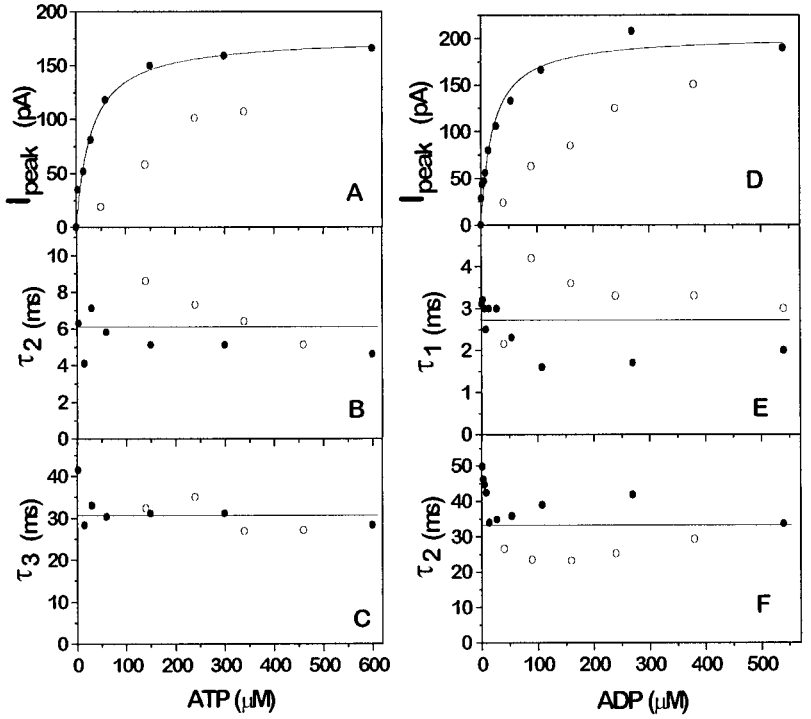

FIGURE 4 BLM experiment: nucleotide dependence of the peak current and the time constants. Conditions: 100 mM NaCl, 20 mM MES (pH 6.2), T = 24°C. ●, Caged nucleotide concentration increased from 5 μM to 2 mM, η = 26%; ○, caged nucleotide 2 mM, η decreased from 30% to 0%. (*A*) ATP dependence of the peak current. (*B*) ATP dependence of τ_2 (decay of transport phase). (*C*) ATP dependence of τ_3 (decay of transport-phase). (*D*) ADP dependence of the peak current. (*E*) ADP dependence of τ_1 (decay of transport phase + slow-release phase). (*F*) ADP dependence of τ_2 (decay of transport phase + slow-release phase).

Inhibition of the AAC by high anion concentration

Mg^{2+} inhibits the transport phase. By further increasing the $MgCl_2$ concentration to 50 mM, the fast-release phase and slow-release phase can also be blocked as shown in Fig. 7 *A* for ADP_{ex}-0_{in}. A small laser artefact that is independent of the presence of the AAC remains. This artefact was found in former experiments to be independent of the investigated protein but related to the illumination of the BLM and to the release of ATP from caged ATP in the vicinity of the membrane (Fendler et al., 1987, 1993). Under ADP_{ex}-0_{in} conditions the transport phase and the slow-release phase overlap and cannot be distinguished. Therefore it is not clear at which Mg^{2+} concentration ADP transport is completely blocked. In Fig. 7 *B* the chloride and $MgCl_2$ dependences, respectively, of the transport phase and slow-release phase are shown normalized to the peak current at 100 mM NaCl. It is found that the slow-release phase as well as the protein-related part of the fast-release phase are inhibited at 200 mM Cl^-.

To discriminate between a Mg^{2+} effect and a chloride effect we repeated the same experiment with NaCl. For ADP_{ex}-0_{in} (Fig. 8 *A*) we found a Cl^- concentration dependence similar to that with $MgCl_2$, i.e., almost complete inhibition at 200 mM Cl^-. In the case of ATP_{ex}-0_{in} (Fig. 8

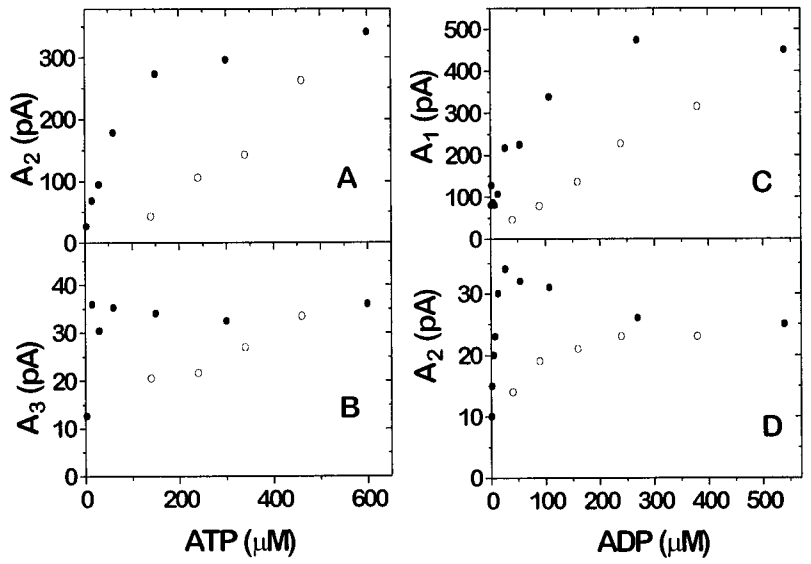

FIGURE 5 BLM experiment (see Fig. 4): corresponding amplitudes of τ_i for ATP_{ex}-0_{in} (*A* and *B*) and ADP_{ex}-0_{in} (*C* and *D*).

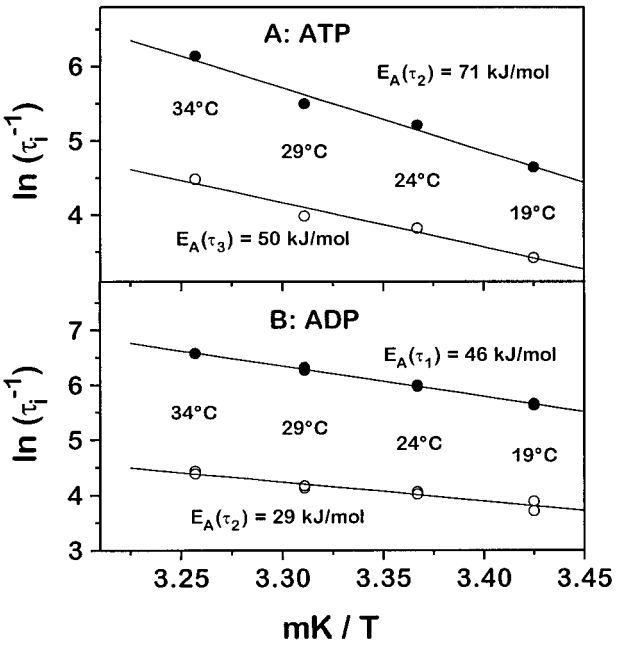

FIGURE 6 BLM experiments: activation energies of τ_2, τ_3 for ATP (*A*: 500 μM caged ATP) and τ_1, τ_2 for ADP (*B*: 500 μM caged ADP) concentration jumps. Conditions: 100 mM NaCl, 20 mM MES (pH 6.2); temperature 19–34°C, η = 26%.

B) the transport phase is blocked at 300 mM NaCl, but the slow-release phase still remains. To clarify the question of whether a specific anionic effect exists, two experiments with ADP_{ex}-0_{in} were carried out: increasing concentration of NaCl and of Na gluconate. The result shows that gluconate blocks less efficiently than chloride (Fig. 9).

Loading of empty liposomes with ADP and ATP

The transient current of the ATP_{ex}-0_{in} and ADP_{ex}-0_{in} transport yields constant amplitudes and relaxation times, even after several flashes. However, in the presence of hexokinase and glucose in the case of ATP_{ex}-0_{in} or creatinephosphokinase and phosphocreatine in the case of ADP_{ex}-0_{in}, a loading of the liposomes with ADP or ATP is observed (Fig. 10). This loading effect is suggested because the shape of the current is similar to the shape of a transient current of the heteroexchange modes, i.e., ATP_{ex}-ADP_{in} and ADP_{ex}-ATP_{in} exchange. At increasing internal nucleotide concentration the amount of transported charge is increased. This is due to the fact that more charge is translocated when the carrier is going through one complete transport cycle. As will be explained in the Discussion, this loading effect yields, in addition to the SSM experiments, substantial evidence for the uniport of ATP and ADP, respectively.

DISCUSSION

ATP and ADP translocation is electrogenic

In previous BLM experiments transient currents induced by ATP and ADP concentration jumps were reported. However, in the case of the ATP_{ex}-0_{in} and ADP_{ex}-0_{in} transport modes it was not quite clear whether electrogenic binding, electrogenic transport, or both are observed in the transient currents. Now we have further evidence for the electrogenic transport of ATP and ADP.

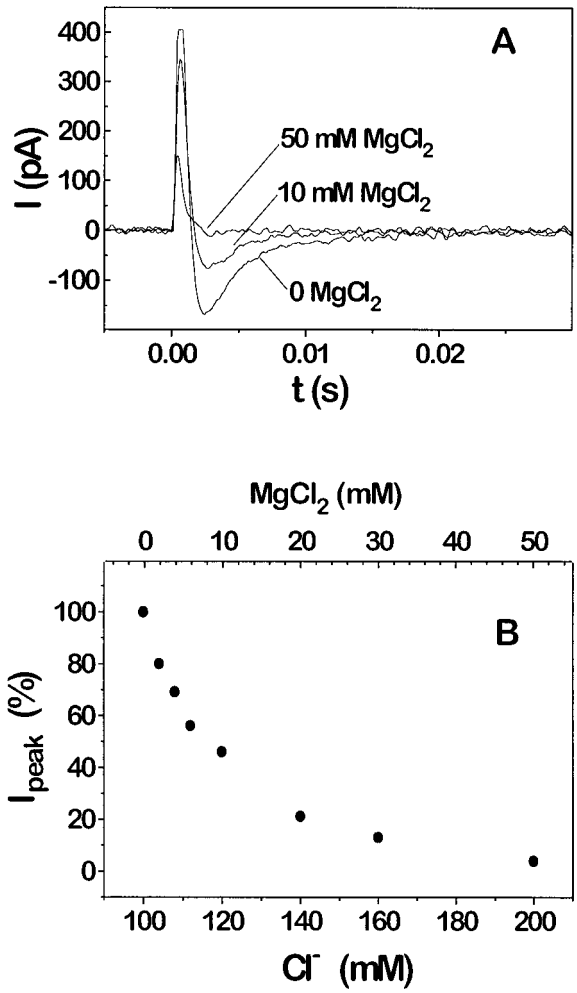

FIGURE 7 BLM experiment: inhibition of an ADP_{ex}-0_{in} signal with $MgCl_2$. (*A*) Transient current traces. (*B*) Peak current of transport phase + slow-release phase at different $MgCl_2$ concentrations; 100 mM NaCl, 20 mM MES (pH 6.2), 200 μM caged ADP; T = 24°C; η = 26%.

The experiments shown in Fig. 10 strongly support the proposed ATP and ADP uniport in the case of unloaded liposomes. The transport of nucleotides into the liposomes could be proved on the addition of hexokinase + glucose (ATP_{ex}-0_{in}) and creatine phosphokinase + phosphocreatine (ADP_{ex}-0_{in}), respectively, to the solution. The effect of hexokinase was already described for the reloading of ADP-loaded liposomes in the ATP_{ex}-ADP_{in} exchange mode (Brustovetsky et al., 1997).

Here, in the case of initially unloaded liposomes, the shape of the transient current changes on the addition of hexokinase and glucose from a simple ATP_{ex}-0_{in} signal to an ATP_{ex}-ADP_{in} signal. The prerequisite for the observation of this heteroexchange signal is the loading of the liposomes with ADP, which in turn requires an initial loading with

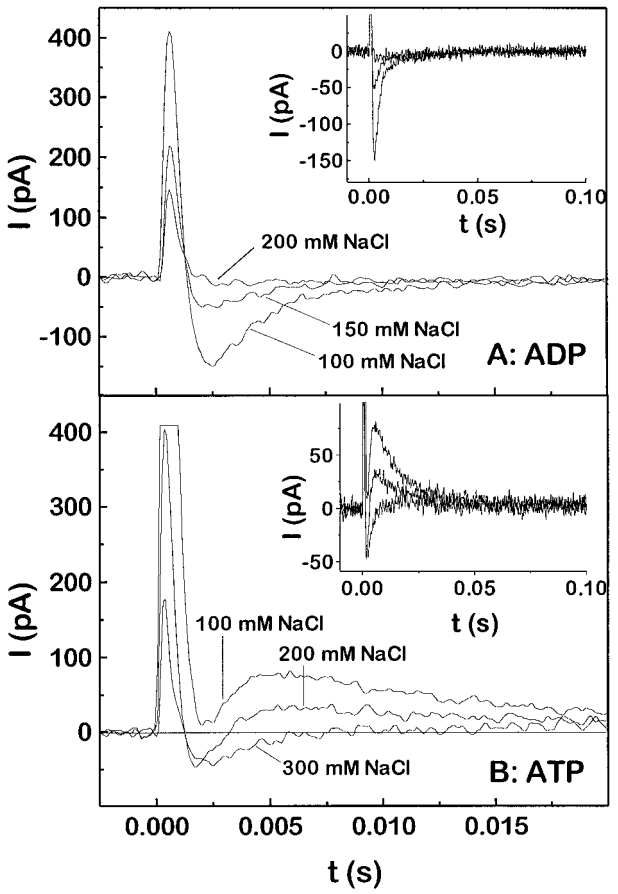

FIGURE 8 BLM experiment: Inhibition of the nucleotide transport at high chloride concentrations. (*A*) ADP_{ex}-0_{in}: 200 μM caged ADP. (*B*) ATP_{ex}-0_{in}: 100 μM ATP. (*Inset*) Larger time scale; 100 mM NaCl, 20 mM MES (pH 6.2); $T = 24°C$; $\eta = 26\%$.

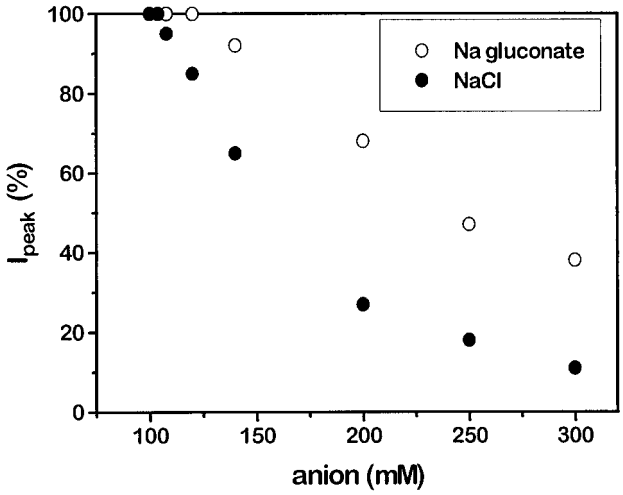

FIGURE 9 BLM experiments: normalized peak current of the transport phase + slow-release phase of an ADP_{ex}-0_{in} signal at different chloride and gluconate concentrations. *Upper trace*: 100–300 mM Na gluconate, 20 mM MES (pH 6.2), 200 μM caged ADP; $T = 24°C$; $\eta = 26\%$. *Lower trace*: 100–300 mM NaCl, 20 mM MES (pH 6.2), 200 μM caged ADP; $T = 24°C$; $\eta = 26\%$.

ATP. This loading with ADP can be explained as follows (see scheme in Fig. 10). After its release from the caged analog, ATP is transported into the liposomes. Because of the low concentration of hexokinase and glucose, the ATP in the solution is converted into ADP relatively slowly, i.e., over the next few minutes. Then the generated ADP in the solution can exchange with the ATP that was translocated into the liposomes, so that the liposomes become loaded with ADP. Now the ATP that was transported out of the liposomes is also converted into ADP, so that after a while there is only ADP present. With the next flash ATP is released, and it can exchange with the ADP inside the liposomes. Consequently, only by assuming that ATP is initially transported into the liposomes in a uniport mode can the loading of the liposomes with ADP in the presence of hexokinase and glucose be explained. In a similar way a net transport of ADP into empty liposomes was shown with creatine phosphokinase and phosphocreatine (Fig. 10 *B*). Taking into account the results from the SSM experiments (Fig. 1, *A* and *C*), an electrogenic ATP and ADP transport is postulated.

An estimation of the internal nucleotide concentration after several flashes yielded a value of 10 μM. This amount of internal ATP or ADP is sufficient to supply the carrier with nucleotides for approximately one turnover. As can be seen in Fig. 10, the amount of transported charge after several flashes is about twice as much as in the completely unloaded state of the liposomes.

For the BLM experiments it is desirable that the liposomes are again nucleotide free before the next flash. This can be accomplished by the following mechanism. After the laser flash only a small fraction of the total caged nucleotide is converted into free nucleotide in the cuvette (~1%). Stirring between the flashes therefore causes a 100-fold dilution of the nucleotide in the vicinity of the membrane (Nagel et al., 1987). Because of the low nucleotide concentration in the solution, the nucleotides that were transported into the liposomes are transported out of the liposomes, yielding virtually nucleotide-free liposomes before the next flash. The maximum amount of internal ATP or ADP after several flashes is in the range of 10 μM (see above). Except for the experiment depicted in Fig. 10, all experiments were carried out in the absence of hexokinase or creatine phosphokinase. Consequently, after several flashes the liposomes were loaded with small amounts of the nucleotide that was released from its caged analog. Because the homoexchange modes (ATP_{ex}-ATP_{in}, ADP_{ex}-ADP_{in}) yield exactly identical results in terms of kinetics compared to the uniport modes (Brustovetsky et al., 1996, and unpublished data), this loading effect is negligible.

The depletion of internal nucleotide after the flash is experimentally supported by the SSM experiments. As shown in Fig. 1, an on-response as well as an off-response is seen because of electrogenic ATP and ADP transport, respectively, whereas the sign of the transported charge was directly opposite in the two cases. The amount of charge

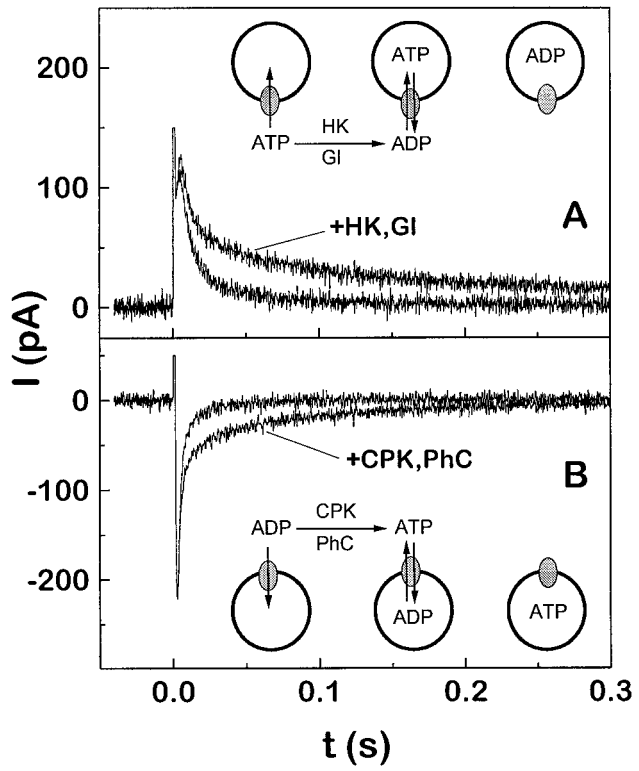

FIGURE 10 BLM experiments: loading of empty liposomes with ADP and ATP. 100 mM NaCl, 20 mM MES (pH 6.2); $T = 24°C$. (*A*) *Lower trace*: 500 μM caged ATP; *upper trace*: 5th flash after the addition of 5 units/ml hexokinase and 1 mM glucose. (*B*) *Upper trace*: 500 μM caged ADP; *lower trace*: 5th flash after the addition of 10 units/ml creatine phosphokinase and 1 mM phosphocreatine. (*Inset*) Schematic model of the loading process (for an explanation see the Discussion).

that is transported during the on- and off-responses is approximately the same (off-response $\approx$ 80–90% of the on-response). Calculations of the ATP or ADP concentration inside the liposomes after one half-cycle of transport activity yielded a value of $\sim$100 μM. Consequently, the internal nucleotide concentration is sufficient for the rebinding and transport of nucleotides out of the liposomes after removal of the nucleotides outside.

The on-response and off-response of the signals (ATP_{ex}-0_{in} and ADP_{ex}-0_{in}) could be blocked by the specific inhibitors CAT and BKA (Fig. 1 *B*). The sign of the transient current corresponds to the transport of negative charge into the liposomes for the ATP on-response (Fig. 1 *C*) and of net positive charge into the liposomes for the ADP on-response (Fig. 1 *A*).

In connection with the transported charge, the question arises if only the protonated nucleotides ($ATPH^{3-}$, $ADPH^{2-}$), the unprotonated nucleotides (ATP^{4-}, ADP^{3-}), or both are transported by the AAC. From previous investigations it was suggested that the unprotonated species are exclusively transported, because the pH dependence of the ADP/ATP exchange is similar to the pH dependence of the fraction of deprotonated nucleotides (Pfaff and Klingenberg, 1968; Brustovetsky et al., 1997). In addition, the absence of H^+ movement accompanying ATP/ADP exchange supports the strict adherence to ATP^{4-} and ADP^{3-} (Wulf et al., 1978).

Further experimental evidence in support of these findings is given by the comparison of transported charge at different pH values in our investigations. Because of the pK of ATP (pK 6.51) and ADP (pK 6.41) for the binding of the first proton, one would expect a relative difference in the ratio of transported charge (Q_{ATP}/Q_{ADP}) in the two uniport modes at pH 6.2 and pH 7.4, which are below and above the pK of the nucleotides. In the SSM experiments we found that within the same experiment (i.e., the same SSM), in the ATP translocation step approximately twice as much charge is transported compared to the ADP translocation ($Q_{ATP}/Q_{ADP} = 2/1$), independent of the pH (pH 6.2 and pH 7.4). Considering the fact that this ratio is not dependent on the pH, we assume that only the unprotonated nucleotides ATP^{4-} and ADP^{3-} are transported. Under this assumption it is concluded that an equivalent of 3.3 countercharges resides in the nucleotide binding site and is cotransported with the nucleotides. This is in agreement with Brustovetsky et al. (1996), who proposed that an equivalent of 3.5 positive countercharges is cotransported with the nucleotides.

Assignment of the transient current phases

The translocation of ATP by the AAC can be blocked by addition of Mg^{2+} (Fig. 1), because MgATP is not transported by the carrier. This allows the differentiation between translocation and other charge movements for the transient signal of the BLM experiments (Fig. 3, *A* and *B*). In the presence of Mg^{2+} a charge movement that is consequently not due to the transport of nucleotides can clearly be identified. Therefore the difference in the signal with and without Mg^{2+} corresponds to the transport of the nucleotides (transport phase). The sign of the current in the transport phase is in agreement with the direction of the current in the SSM experiment. In the case of ATP_{ex}-0_{in}, the transport phase represents the translocation of negative charge into the liposomes and in the case of ADP_{ex}-0_{in} of positive charge into the liposomes.

On inhibition of the transport phase by Mg^{2+}, two phases remain unaffected in both cases (ATP_{ex}-0_{in}, ADP_{ex}-0_{in}), namely the fast-release phase and the slow-release phase. The fast-release phase corresponds to a negative charge movement toward the inside of the liposomes or a positive charge movement in the opposite direction. It is too fast to be resolved. It might be due to the release of a proton ($k > 10^5\ s^{-1}$) in the photolytic nucleotide release reaction (Walker et al., 1988). The slow-release phase corresponds to the movement of positive charge toward the binding site, and the amount of transported charge is equal to or smaller than that in the fast-release phase. From the pH dependence of $\tau_{1,Mg^{2+}}$ (Tables 1 and 2) and the comparison with spectroscopic data it can be concluded that $\tau_{1,Mg^{2+}}$ represents the release of the nucleotides, which is accompanied by a

charge movement. In addition, the local pH in the binding site has to be similar to the pH in the solution, because the release of the nucleotides is proposed to take place in the binding site (see below), and the time constant for nucleotide release at pH 6.2 is equal to the time constant for nucleotide release in the bulk solution. This fact suggests that with respect to H^+ the binding site is in free exchange with the bulk phase. Because the pK of the fixed charges of the carrier is not known, it is not clear whether there is an effect on the local pH from this side.

After inhibition with CAT/BKA, both the fast-release phase and the slow-release phase are blocked, and only the laser artefact remains (Fig. 3 *C* and *D*). CAT binds selectively to the AAC in the cytosolic state (Fig. 11 *A*) and cannot permeate the membrane. BKA, however, can permeate the membrane and binds to the matrix state of the carrier (Weidemann et al., 1970; Klingenberg, 1985). CAT and BKA block the corresponding binding site, so that nucleotides or caged nucleotides can no longer bind.

At high chloride concentration (see Fig. 8) the fast-release phase can be blocked in both cases (ATP_{ex}-0_{in}, ADP_{ex}-0_{in}), and the slow-release phase only in the case of ADP_{ex}-0_{in}. The reason why the slow-release phase in the case of ATP_{ex}-0_{in} is not inhibited is unclear. A tentative explanation could be that in the binding site the Cl^- activity is reduced because of the presence of a negative charge due to ATP binding.

By applying concentration jumps with different ATP concentrations, a half-saturating value of 60 μM was found in the SSM experiment (Fig. 2). However, according to our assumption that only the unprotonated fraction of ATP (~30%, pK 6.51; Martell and Smith, 1974) is transported by the carrier, the half-saturation concentration for ATP has to be corrected to ~20 μM. This is still a relatively high value compared to literature values (3 μM; Klingenberg, 1976) and to BLM measurements with nucleotide-loaded liposomes (unpublished results), which yield values in the range of $K_{0.5} \approx 10$ μM for the ATP binding. The difference in the affinity might be due to different experimental conditions, for example, the absence of nucleotides inside the liposomes in the steady-state experiments.

Transport model

For the interpretation of the data it has to be assumed that caged ATP binds to the carrier, which is in line with previous studies (Brustovetsky et al., 1996). On the basis of our results and referring to Fig. 11 *C*, we propose the following model for nucleotide binding and transport by the AAC: caged ATP $C_o \rightarrow$ caged ATP* $C_o \rightarrow$ ATP $C_o \rightarrow C_i$ + ATP. Caged ATP is bound to the carrier, and according to the data the dissociation rate is probably slow. After the laser flash, ATP is released from the prebound caged ATP in the binding site and is transported through the carrier without exchanging with the solution. For ADP the same mechanism is applicable. We call this mechanism *release in site*.

In Fig. 11 *C* the reaction pathways for ADP and ATP translocation in the case of the BLM experiment are sche-

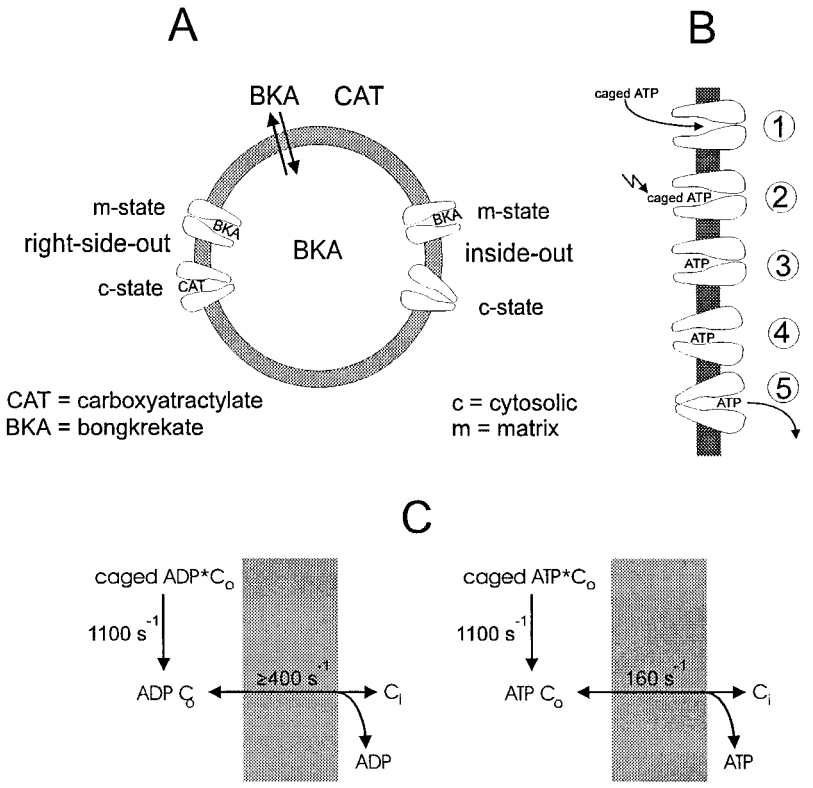

FIGURE 11 (*A*) Inhibition by CAT and BKA. BKA can permeate the membrane and inhibits the carrier in the matrix state (m-state), whereas CAT cannot permeate the membrane and inhibits the carrier in the cytosolic state (c-state). The two states symbolize the orientation of the binding site with respect to the matrix space and the cytosol in the native system. (*B*) Release-in-site mechanism for ATP (ADP is analogous). (*1*) binding of caged ATP, (*2*) laser flash, (*3*) release of ATP from prebound caged ATP in the binding site, (*4*) conformational transition of the carrier, (*5*) release of ATP into the liposome. (*C*) Schematic model of ADP and ATP translocation in the BLM experiments. *, caged nucleotide that has absorbed a photon.

matically depicted. It is similar to a model already proposed for the NaK-ATPase (Fendler et al., 1994). However, for the NaK-ATPase rapid exchange of the nucleotides in the binding site and in solution was assumed. Caged ATP* represents caged ATP that has already absorbed a photon and will release the nucleotide with a time constant of ~1 ms at pH 6.2 (see Materials and Methods).

The first and most obvious interpretation of the nucleotide dependence of the peak current (Fig. 4) would be the competitive binding of nucleotides and caged nucleotides to the AAC as has already been described for the NaK-ATPase (Fendler et al., 1993; Nagel et al., 1987). This is supported by the fact that caged nucleotides bind to the AAC binding site with a affinity similar to that for nucleotides but are not transported by the carrier (Brustovetsky et al., 1997). Under these assumptions a nucleotide concentration-dependent relaxation time should be obtained. However, no ATP or ADP dependence of the time constants (τ_2, τ_3 and τ_1, τ_2) was observed in the experiments.

Therefore, an alternative interpretation involving the release-in-site mechanism is proposed (Fig. 11 *B*). In this mechanism competitive binding of caged ATP and ATP has no effect on the initial reaction after the flash, which can be explained as follows. No ATP-dependent time constant was found, so that it has to be concluded that nucleotide binding is not a rate-limiting process under the given experimental conditions. Therefore, at increasing caged ATP concentration (Fig. 4, *filled circles*), the peak current can only be increased by increasing the number of activated AAC molecules. A hyperbolic fit to the caged ATP dependence of the peak currents yields half-saturating concentrations of $K_{0.5}$(cATP) = 104 μM and $K_{0.5}$(cADP) = 78 μM (Fig. 4, *A* and *D*). The release-in-site mechanism also explains the linear behavior of the peak current at varying η and constant caged nucleotide concentration (Fig. 4, *A* and *D*, *open circles*). At a caged nucleotide concentration of ~2 mM, the peak current is in saturation. All of the available binding sites are assumed to be oriented toward the outside of the liposomes. At decreasing η and constant caged nucleotide concentration, the number of activated carrier molecules in the first instance is proportional to η, yielding a linear nucleotide dependence. A slight curvature of these data might indicate overlapping activation from the bulk solution, with competition between nucleotides and caged nucleotides.

Following this interpretation, nucleotides and caged nucleotides compete for the binding site. However, this competitive binding has no influence on the peak current, because the peak current is determined by the initial half-cycle of the reaction, which is initiated by release in site. This does not rule out the possibility that competitive binding is of importance in the steady state.

Kinetics of the ATP and ADP translocation

Because the time resolution of the rapid solution exchange technique on the basis of the SSM is significantly below the time resolution that is achieved by the use of caged compounds in the BLM technique (10 ms compared to 1 ms), only the BLM data were used for the analysis of the AAC kinetics. For the assignment of the time constants the following criteria were applied: ATP dependence of the time constants and the corresponding amplitudes, pH dependence, and temperature dependence. The general approach to the assignment of certain time constants to the nucleotide translocation is by exclusion of all other possible assignments.

ATP translocation

In the BLM experiments three time constants were found for the transport phase in the case of ATP_{ex}-0_{in}: $\tau_1 \approx 1$ ms, $\tau_2 \approx 6$ ms, and $\tau_3 \approx 30$ ms. τ_1 is most probably determined by the release of ATP in the binding site, τ_2 by the ATP translocation through the carrier, and τ_3 cannot be related to the AAC (see below).

The conclusion that τ_1 is determined by the photolytic release of ATP, which is ~0.9 ms at pH 6.2, is supported by experiments at varying pH and by comparison with spectroscopic data (Table 2). At pH 6.2 τ_1 is in agreement with the time constant for ATP release. At pH 7.2 the time constants of the transport phase are τ_1 = 6.3 ms and τ_2 = 8.3 ms. This can be explained as follows. At pH 6.2 the rise of the transport phase ($\tau_1 \approx 1$ ms) is determined by the release of ATP from caged ATP. When the pH is increased to 7.2 the time constant for the ATP release also increases by a factor of $\sim 10^{\Delta pH} = 10$. This yields a time constant for ATP release of ~8.6 ms, so that at pH 7.2 the ATP release is slower than the ATP translocation (~6 ms), which is pH independent. Therefore, at pH 7.2 the ATP transport is faster and appears as τ_1 = 6.3 ms and the ATP release as τ_2 = 8.3 ms, which is in good agreement with the expected value of 8.6 ms. After the inhibition of the transport phase by Mg^{2+}, the release of ATP could still be observed in the decay of the slow-release phase. As can be seen in Table 2, $\tau_{1,Mg^{2+}}$ is almost equal to the time constant of the ATP release at 4 mM Mg^{2+} obtained by spectroscopic experiments.

The fact that we observed the time constant for ATP release in our signals even at high ATP concentrations further supports the release-in-site model. If the ATP were bound from the solution, one would expect to observe an ATP-dependent time constant that becomes fast at highly saturating ATP concentrations.

Because τ_1 corresponds to the nucleotide release in the binding site, either τ_2 or τ_3 has to be the rate-limiting step in the electrogenic transport of ATP. As will be explained below, τ_3 cannot be assigned to the protein. Consequently, the time constant τ_2 most probably represents the electrogenic ATP translocation by the carrier, with a corresponding reaction rate constant of $\tau_2^{-1} = k_{2,ATP} \approx 160\ s^{-1}$. Neither τ_2 nor τ_3 is ATP dependent (Fig. 4), so that ATP binding is assumed to be fast. As can be seen from the ATP dependence of the amplitudes (Fig. 5, *A* and *B*), A_2, which

corresponds to τ_2, determines the ATP dependence of the peak current, whereas A_3 does not exhibit any characteristic ATP dependence. If the peak current is increased by activating more carrier molecules, one would expect the two amplitudes to increase in the same way. This is not the case for A_3, so that τ_3 cannot be identified as a protein-related time constant. τ_3 could also represent the system time constant of the compound membrane. However, the amplitude of the system time constant should be proportional to the amount of translocated charge, which is also not the case.

Because ATP binding has to be faster than τ_2, τ_2 corresponds to a following reaction step that is the ATP translocation itself or a preceding rate-limiting step. From the current measurements we cannot distinguish between these two cases, and we call the τ_2-related partial reaction ATP translocation. The activation energy for τ_2 is 71 kJ/mol (Fig. 6 *A*), which is in fair agreement with the values from the steady-state experiments (58 kJ/mol; Klingenberg, 1976).

ADP translocation

In the case of ADP_{ex}-0_{in} no explicit assignment of the time constants can be made, but a lower limit for the reaction rate constant of the ADP translocation is determined. The time constants are $\tau_1 \approx 2$–3 ms and τ_2 ranging from 10 to 50 ms (Table 1, Fig. 4, *E* and *F*).

At pH 6.2, $\tau_1 \approx 2$–3 ms can either be assigned to the ADP translocation or to the ADP release. If the ADP translocation determines τ_1, the reaction rate constant for this process is $\tau_1^{-1} \approx 400\ s^{-1} = k_{1,ADP}$. If the ADP release is rate limiting, τ_1^{-1} yields a lower limit for the ADP translocation, i.e., $k_{1,ADP} \geq 400\ s^{-1}$. τ_2 cannot be assigned to the protein, and it is not a system time constant, for the same reason as τ_3 in the case of ATP_{ex}-0_{in}.

$\tau_{1,Mg^{2+}}$ is observed after blocking of the transport phase by Mg^{2+}, and it shows a significant pH dependence (Table 1), as does τ_1. Comparison with the spectroscopic data at 0 and 4 mM Mg^{2+} shows that τ_1 and $\tau_{1,Mg^{2+}}$ are determined by the release of ADP from caged ADP at higher pH (pH 6.65 and pH 7.0). At pH 6.2 τ_1 and $\tau_{1,Mg^{2+}}$ were in the range of 2 ms, and the release of ADP was ~1 ms. No explicit assignment of the two time constants can be made because either ADP release or ADP translocation or both could be in the time range of 1–2 ms. On the one hand, the activation energy of τ_1 (46 kJ/mol) is very similar to that of the ADP release (57 kJ/mol), which suggests an assignment of τ_1 to the release of ADP. On the other hand, the value for τ_1 is twice as large as the time constant for ADP release, which might indicate that τ_1 represents ADP translocation. Taking these arguments together, τ_1^{-1} yields a lower limit for the ADP transport rate.

The function of the AAC is symmetrical

After inhibition with CAT, which blocks only the cytosolic site (c-site) of the carrier (Fig. 11 *A*; Brustovetsky et al., 1996), in an ATP_{ex}-0_{in} experiment the peak current is reduced to ~50%, implying that the AAC is probably randomly incorporated into the liposomes, i.e., that 50% are inside-out and right-side-out oriented. The values for the time constants τ_2 and τ_3 (results not shown) after inhibition with CAT are in agreement with the values without CAT. From this we conclude that there is no significant kinetic difference between the two transport directions, and as a first approximation, the AAC can be regarded as symmetrical.

Inhibition of the AAC by anions

In Figs. 7 *A* and 8 *A* it is demonstrated that all three phases of the transient current in the case ADP_{ex}-0_{in} can be blocked at high chloride concentrations (200 mM). Fig. 9 further proves that it is an anionic effect because two anions, chloride and gluconate, with the same charge inhibit with different efficiencies. This is in agreement with the observation that caged ATP binds more efficiently to the AAC in a gluconate medium than in a chloride medium (data not shown). In the case of ATP_{ex}-0_{in} the fast-release phase was significantly reduced at 300 mM Cl^-, but the slow-release phase could still be observed. The reason for this finding is unclear.

Inhibition of the AAC carrier by anions could be explained by the shielding of the positive charges in the carrier-binding site, which are believed to be responsible for nucleotide binding. Similar results were found for the NaK-ATPase by Nørby and Esmann (1997).

CONCLUSIONS

In the system ATP_{ex}-0_{in} and ADP_{ex}-0_{in}, ATP and ADP are electrogenically transported into the liposomes by the AAC. The charge movements in the system ATP_{ex}-0_{in} and ADP_{ex}-0_{in} have opposite directions. This supports the model of an equivalent of 3.3 positive countercharges at the binding site of the AAC, resulting in -0.7 and $+0.3$ net transported charges in the cases ATP_{ex}-0_{in} and ADP_{ex}-0_{in}, respectively. The transport of the nucleotides could be inhibited by CAT/BKA and by Mg^{2+}. A reaction rate constant for the ATP translocation of 160 s^{-1} and a lower limit for the ADP translocation of 400 s^{-1} were determined. The function of the carrier was found to be approximately symmetrical. The release of the nucleotides could be observed in the transient electrical signal. As a model we propose that the nucleotides are released in the binding site from the prebound caged nucleotides and then translocated by the carrier (here for ATP): caged ATP $C_o \rightarrow$ caged ATP* $C_o \rightarrow$ ATP $C_o \rightarrow$ C_i + ATP. The nucleotide binding and transport by the AAC can be blocked by anions.

We thank Dr. R. J. Clarke for reviewing the manuscript.

This work was supported by the Deutsche Forschungsgemeinschaft (SFB 472).

REFERENCES

Bamberg, E., H.-J. Apell, N. A. Dencher, W. Sperling, H. Stieve, and P. Läuger. 1979. Photocurrents generated by bacteriorhodopsin on planar bilayer membranes. *Biophys. Struct. Mech.* 5:277–292.

Borlinghaus, R., H.-J. Apell, and P. Läuger. 1987. Fast charge translocations associated with partial reactions of the Na,K pump. I. Current and voltage transients after photochemical release of ATP. *J. Membr. Biol.* 97:161–178.

Brustovetsky, N., E. Bamberg, T. Gropp, and M. Klingenberg. 1997. Biochemical and physical parameters of the electrical currents measured with the ADP/ATP carrier by photolysis of caged ADP and ATP. *Biochemistry.* 36:13865–13872.

Brustovetsky, N., A. Becker, M. Klingenberg, and E. Bamberg. 1996. Electrical currents associated with nucleotide transport by the reconstituted mitochondrial ADP/ATP carrier. *Proc. Natl. Acad. Sci. USA.* 93:664–668.

Dancshazy, Z., and B. Karvaly. 1976. Incorporation of bacteriorhodopsin into a bilayer lipid membrane: a photoelectric-spectroscopic study. *FEBS Lett.* 72:136–138.

Fendler, K., E. Grell, and E. Bamberg. 1987. Kinetics of pump currents generated by the Na^+,K^+-ATPase. *FEBS Lett.* 224:83–88.

Fendler, K., S. Jaruschewski, A. Hobbs, W. Albers, and J. P. Froehlich. 1993. Pre-steady state charge translocation in NaK-ATPase from eel electric organ. *J. Gen. Physiol.* 102:631–666.

Fendler, K., S. Jaruschewski, J. P. Froehlich, W. Albers, and E. Bamberg. 1994. Electrogenic and electroneutral partial reactions in Na^+K^+-ATPase from eel electric organ. *In* The Sodium Pump. E. Bamberg und W. Schoner, editors. Steinkopf, Darmstadt, Germany. 495–506.

Klingenberg, M. 1972. ATP synthesis and adenine nucleotide transport in mitochondria. *In* Mitochondria/Biomembranes: Proceedings of the 8th FEBS Meeting in Amsterdam. Elsevier, Amsterdam. 147–162.

Klingenberg, M. 1976. The ADP-ATP carrier in mitochondrial membranes. *In* The Enzymes of Biological Membranes: Membrane Transport, Vol. 3. A. N. Martonosi, editor. Plenum Publishing, New York and London. 383–438.

Klingenberg, M. 1980. The ATP, ADP translocation in mitochondria, a membrane potential controlled transport. *J. Membr. Biol.* 56:97–105.

Klingenberg, M. 1985. The ADP/ATP carrier in mitochondrial membranes. *In* The Enzymes of Biological Membranes: Bioenergetics of Electron and Proton Transport, Vol. 4, 2nd Ed. A. N. Martonosi, editor. Plenum, New York. 511–553.

Knoll, W., and G. Stark 1977. Temperature-jump experiments on thin lipid membranes in the presence of valinomycin. *J. Membr. Biol.* 37:13–28.

Krämer, R. 1986. Reconstitution of ADP/ATP translocase in phospholipid vesicles. *In* Biomembranes. Part M: Transport in Bacteria, Mitochondria, and Chloroplasts—General Approaches and Transport Systems. Section III: Transport in Mitochondria and Chloroplasts. S. Fleischer and B. Fleischer, editors. *Methods Enzymol.* 125:610–618.

Martell, A. E., and R. M. Smith. 1974. Critical Stability Constants, Vol. 1: Amino Acids. Plenum Press, New York and London. 281–284.

Nagel, G., K. Fendler, E. Grell, and E. Bamberg. 1987. Na^+ currents generated by the purified (Na^+ + K^+)-ATPase on planar lipid membranes. *Biochim. Biophys. Acta.* 901:239–249.

Nørby, J. G., and M. Esmann. 1997. The effect of ionic strength and specific anions on substrate binding and hydrolytic activities of Na,K-ATPase. *J. Gen. Physiol.* 109:555–570.

Pfaff, E., and M. Klingenberg 1968. Adenine nucleotide translocation of mitochondria. I. Specificity and control. *Eur. J. Biochem.* 6:66–79.

Pintschovius, J., and K. Fendler. 1999. Charge translocation by the Na^+K^+-ATPase investigated on solid supported membranes. Part I. Rapid solution exchange—a new technique discussed. *Biophys. J.* 76: 814–826.

Walker, J. W., G. P. Reid, J. A. McCray, and D. R. Trentham. 1988. Photolabile 1-(2-nitrophenyl)ethyl phosphate esters of adenine nucleotide analogues. Synthesis and mechanism of photolysis. *J. Am. Chem. Soc.* 110:7170–7177.

Weidemann, M. J., H. Erdelt, and M. Klingenberg. 1970. Effect of bongkrekic acid on the adenine nucleotide carrier in mitochondria: tightening of adenine nucleotide binding and differentiation between inner and outer sites. *Biochem. Biophys. Res. Commmun.* 39:363–370.

Wulf, R., A. Kaltstein, and M. Klingenberg. 1978. H^+ and cation movements associated with ADP/ATP transport in mitochondria. *Eur. J. Biochem.* 82:585–592.